Received October 17, 2020, accepted October 27, 2020, date of publication October 29, 2020, date of current version November 11, 2020.

Digital Object Identifier 10.1109/ACCESS.2020.3034712

Non-Singular Fast Terminal Sliding Mode Control With Disturbance Observer for Underactuated Robotic Manipulators

SALEH MOBAYEN[1,2], (Member, IEEE), SOHEILA MOSTAFAVI[2], AND AFEF FEKIH[3], (Senior Member, IEEE)
[1]Future Technology Research Center, National Yunlin University of Science and Technology, Douliou 64002, Taiwan, R.O.C.
[2]Electrical Engineering Department, Faculty of Engineering, University of Zanjan, Zanjan 45371-38791, Iran
[3]Department of Electrical and Computer Engineering, University of Louisiana at Lafayette, Lafayette, LA 70504-3890, USA

Corresponding author: Saleh Mobayen (mobayens@yuntech.edu.tw)

ABSTRACT This paper proposes a novel non-singular fast terminal sliding control technique for underactuated robotic manipulators. The proposed approach combines the robustness properties of sliding mode-based control approaches with the approximation accuracy of disturbance observers to suppress both matched and mismatched uncertainties. It also solves the singularity and complex-value number problems associated with fast terminal sliding mode control (FTSMC), while guaranteeing fast convergence rate, robustness and tracking accuracy. The performance of the proposed approach is assessed using a three-link underactuated robotic manipulator with and without holding brakes. The obtained results confirmed the fast convergence rate of the disturbance approximation and position tracking errors along with the excellent robustness and dynamic performance of the proposed control approach. Additionally, due to the estimation properties of the disturbance observer, fast and excellent tracking performance was achieved without the use of large feedback gains.

INDEX TERMS Underactuated robotic systems, fast terminal sliding mode control, non-singular control, disturbance observer, finite-time convergence.

I. INTRODUCTION

Control of underactuated mechanical systems has been an active research area over the last decades. These systems have attractive features such as reduced bulkiness, lighter weight and cheaper cost [1], and have widespread applications in various systems spanning from overhead cranes [2], under-water vehicles [3], space robots [4], vertical take-off and landing drones [5], inverted pendulums [6], aircraft assembly systems [7], 3D bipedal robots [8], proprioceptive tactile sensing [9], to hovercrafts [10]. These systems can either be underactuated by design [11] or because of component failures. The facts that they have fewer actuators than the degrees of freedom to be controlled, however, results in both theoretical and practical control challenges [12]. The first design approach for a class of underactuated and non-mimnimum phase systems was proposed by Spong in [13]. That design procedure combined partial nonlinear feedback linearization with saturation function-based Lyapunov techniques to stabilize the closed-loop system without the need for stable zero dynamics. The study proposed by Olfati-Saber [14] exploited the physical structure of underactuated systems, typically appearing in robotic and aerospace systems, such as motion symmetry, actuated variables, and inputs to transform these latter into cascaded nonlinear systems with structural features that are suitable for the control goals.

It is worth noting, however, that a large class of underactuated robotic systems cannot be controlled by smooth feedback if the Brockett's necessary conditions are not satisfied [15]. Hence, the high-frequency control nature of sliding mode control (SMC) has resulted in its recent consideration in the control/tracking of underactuated robotic manipulators. Additionally, SMC is one of the main approaches to control uncertain systems [16]. The design methodology suppresses the uncertainties by exactly keeping the sliding variable at zero. This is accomplished via two phases, the reaching

The associate editor coordinating the review of this manuscript and approving it for publication was Shihong Ding.

and sliding phase. In the sliding phase, a sliding surface is designed so that the system represents the desired dynamic behavior. In the reaching phase, a controller is applied to force the tracking errors/state trajectories to remain on the sliding surface [17]. During the reaching phase of standard SMC, the system is not robust and thus can be destabilized by the matched disturbances. Essentially, the robust tracking action is done only after the tracking errors reach the switching surface, and thus robust performance is not contented throughout the reaching mode [18]. In global sliding mode control (GSMC) schemes, the reaching phase is omitted and the state errors start moving on the sliding manifold from the beginning via an extra term in the switching surface [19]. Nevertheless, standard sliding mode control does not guarantee convergence in finite time. To alleviate this problem, terminal sliding mode (TSMC) and fast terminal sliding mode control (FTSM) approaches have been suggested [20], [21]. TSMC technique drives the tracking errors to the equilibrium in finite time via a fractional power in the switching surface [22]. Though, TSMC offers improved features such as tracking precision and robust performance compared to SMC, it suffers from the singularity issue, which results in high-amplitude control signals. Additionally, when the error trajectories are far away from the origin, TSMC has slow convergence rates. To solve these problems, non-singular FTSM control schemes [23] were proposed to ensure rapid convergence, high-precision and avoid singularity. In [24], a global non-singular TSMC design was proposed for rigid robotic manipulators where the time taken to reach the origin from any initial condition was guaranteed to be finite. In [25], a hierarchical TSMC approach was proposed for nonlinear underactuated systems that ensured that the tracking error is derived to the origin in finite time. A trajectory tracking control design for underactuated autonomous surface vessels was proposed in [26]. It combined trajectory planning and non-singular TSMC methods to design two global finite-time stabilizers for position tracking of surface vessels. However, the proposed TSMC [26] was only designed for a special class of underactuated systems and was not generalized to a large class of underactuated systems. Reference [27] discussed the design of a non-singular FTSM controller for the underactuated spacecraft system in which the nonlinear dynamics are linearized about the circular reference orbits. The FTSM-based control design was proposed in [28] for uncertain underactuated systems with disturbances.

To suppress both the matched and mismatched uncertainties and eliminate external disturbances, disturbance observer-based approaches, have recently emerged as a viable solution [15], [29], [30]. These observer-based designs were shown to provide globally asymptotically stable and locally exponentially stable path following errors in underactuated systems [31]. An observer-based sliding mode control approach was proposed in [32] for underactuated overhead cranes suffering from both matched and unmatched disturbances. The design was shown to ensure satisfactory control performance even when the crane works under unfavorable conditions. An adaptive SMC methodology based on nonlinear disturbance observer was proposed in [33] for the depth tracking problem of autonomous underwater vehicles. A composite super-twisting SMC control based on a novel disturbance observer was proposed in [34] for the speed regulation of PMSM. The disturbance observer-based fast terminal sliding controllers were successfully implemented in [35], [36]. Some of the above approaches, however, suffered from the chattering problem whereas others suffered from the singularity problem.

To the best of our knowledge, no efforts have been made for the design of non-singular FTSM controller based on disturbance observer and GSMC for tracking control of underactuated robot manipulators with unknown bounded external disturbances.

Based on the above discussion, we propose in this paper a disturbance observer-based non-singular FTSM control design for underactuated robotic manipulators. The main contributions of this paper are as follows:

- A design approach that combines the robustness properties of sliding mode-based control approaches with the approximation accuracy of disturbance observers to suppress both matched and mismatched uncertainties
- A control technique that solves the singularity and complex-value number problems of FTSMC, while guaranteeing fast convergence rate, robustness and tracking accuracy.
- A global sliding mode control scheme that completely removes the effects of external disturbances, even when their bounds are unknown. Hence, guaranteeing robust performance right from the beginning.

The remainder of this article is organized as follows. In Section 2, the problem formulation and necessary preliminaries are introduced. The design procedures for the disturbance observer and non-singular FTSMC controller are given in section 3. Simulation results illustrating the performance of the proposed design on a three-link underactuated robotic manipulator are illustrated in section 4. Lastly, concluding remarks are provided in Section 5.

II. PROBLEM FORMULATION

Consider the Euler–Lagrange dynamic equation of an m-link robotic manipulator as [37]

$$\bar{\boldsymbol{B}}\left(\bar{q}\right)\ddot{\bar{q}} + \boldsymbol{C}\left(\bar{q},\, \dot{\bar{q}}\right)\dot{\bar{q}} + \bar{g}\left(\bar{q}\right) = \bar{u}\left(t\right), \tag{1}$$

where $\bar{q} \in R^m$, $\dot{\bar{q}} \in R^m$, $\ddot{\bar{q}} \in R^m$ signify the position, velocity and acceleration vectors of joints, correspondingly; $\bar{u}\left(t\right) = \left[u_1 \cdots u_n \cdots u_m\right]^T \in R^m$ means the control signal denoting the torque applied on joints; $\bar{\boldsymbol{B}}\left(\bar{q}\right) \in R^{m\times m}$ indicates the positive-definite bounded inertia matrix; $\boldsymbol{C}(\bar{q}, \dot{\bar{q}}) \in R^{m\times m}$ signifies the centripetal-Coriolis matrix; $\bar{g}(\bar{q}) \in R^m$ designates the gravity vector. Considering $\bar{\tau}_d(\bar{q}, \dot{\bar{q}}) \in R^m$ as the disturbance vector, $\bar{\boldsymbol{f}}_{\boldsymbol{d}} \in R^{m\times m}$ as the dynamic friction coefficient matrix and $\bar{\boldsymbol{f}}_s \in R^m$ as the static friction vector, the complete dynamical model of the m-link robotic manipulator is described by [38]:

$$\bar{B}(\bar{q})\ddot{\bar{q}}+C(\bar{q},\dot{\bar{q}})\dot{\bar{q}}+\bar{g}(\bar{q})+\bar{f}_d\dot{\bar{q}}+\bar{f}_s(\dot{\bar{q}})+\bar{\tau}_d(\bar{q},\dot{\bar{q}})=\bar{u}(t). \tag{2}$$

The inertia matrix $\bar{B}(\bar{q})$ can be expressed as:

$$\bar{B}(\bar{q}) = B(\bar{q}) + \Delta B(\bar{q}), \tag{3}$$

where $B(\bar{q})$ and $\Delta B(\bar{q})$ illustrate the known and unknown parts of $\bar{B}(\bar{q})$, correspondingly. The dynamic system (2) is rewritten by:

$$\bar{B}(\bar{q})\ddot{\bar{q}}+n(\bar{q},\dot{\bar{q}})+\bar{f}_d\dot{\bar{q}}+\bar{f}_s(\dot{\bar{q}})+\bar{\tau}_d(\bar{q},\dot{\bar{q}})=\bar{u}(t) \tag{4}$$

where $n(\bar{q},\dot{\bar{q}}) = C(\bar{q},\dot{\bar{q}})\dot{\bar{q}} + \bar{g}(\bar{q})$. Hence, in the existence of parametric uncertainties and disturbances, and considering $n(\bar{q},\dot{\bar{q}}) = n_0(\bar{q},\dot{\bar{q}}) + \Delta n(\bar{q},\dot{\bar{q}})$, with $n_0(\bar{q},\dot{\bar{q}})$ as the known part of $n(\bar{q},\dot{\bar{q}})$ and $\Delta n(\bar{q},\dot{\bar{q}})$ as the unknown part of $n(\bar{q},\dot{\bar{q}})$, the dynamical equation (4) can be written as [39]:

$$\begin{aligned}\ddot{\bar{q}} = -B(\bar{q})^{-1}\{&n_0(\bar{q},\dot{\bar{q}})+\bar{f}_d\dot{\bar{q}}+\bar{f}_s(\dot{\bar{q}})\\ &+\bar{\tau}_d(\bar{q},\dot{\bar{q}})+\Delta B(\bar{q})\ddot{\bar{q}}+\Delta n(\bar{q},\dot{\bar{q}})-\bar{u}(t)\}\end{aligned} \tag{5}$$

From (5), the simplified dynamical model of an m-link robotic manipulator is expressed as:

$$\ddot{\bar{q}} = B(\bar{q})^{-1}\bar{u}(t) + \bar{D}(t) + \bar{f}(\bar{q},\dot{\bar{q}}), \tag{6}$$

where $\bar{D}(t) = -B(\bar{q})^{-1}\{\bar{f}_d\dot{\bar{q}}+\bar{f}_s(\dot{\bar{q}})+\bar{\tau}_d(\bar{q},\dot{\bar{q}})+\Delta B(\bar{q})\ddot{\bar{q}}+\Delta n(\bar{q},\dot{\bar{q}})\}$ denotes the lumped uncertainties and disturbances and $\bar{f}(\bar{q},\dot{\bar{q}}) = -B(\bar{q})^{-1}n_0(\bar{q},\dot{\bar{q}})$ represents the bounded known nonlinear function. The dynamics (6) can also be written in matrix form as:

$$\ddot{\bar{q}} = \begin{bmatrix}\ddot{q}_1\\ \vdots\\ \ddot{q}_n\\ \vdots\\ \ddot{q}_m\end{bmatrix} = \begin{bmatrix}M_0 & M_1\\ M_2 & M_3\end{bmatrix}\begin{bmatrix}u_1\\ \vdots\\ u_n\\ \vdots\\ u_m\end{bmatrix} + \begin{bmatrix}D_1\\ \vdots\\ D_n\\ \vdots\\ D_m\end{bmatrix} + \begin{bmatrix}f_1(\bar{q},\dot{\bar{q}})\\ \vdots\\ f_n(\bar{q},\dot{\bar{q}})\\ \vdots\\ f_m(\bar{q},\dot{\bar{q}})\end{bmatrix}, \tag{7}$$

where $M_0 \in R^{n\times n}$, $M_1 \in R^{n\times r}$, $M_2 \in R^{r\times n}$ and $M_3 \in R^{r\times r}$ are submatrices of $B(\bar{q})^{-1}$. Assuming r to be the number of passive joints and n the number of active joints of the m-link robotic manipulator, the dynamical equation of the underactuated system can be re-written as:

$$\begin{bmatrix}\ddot{q}_1\\ \vdots\\ \ddot{q}_n\\ \vdots\\ \ddot{q}_m\end{bmatrix} = \begin{bmatrix}M_0 & M_1\\ M_2 & M_3\end{bmatrix}\begin{bmatrix}u_1\\ \vdots\\ u_n\\ 0\\ \vdots\\ 0\end{bmatrix} + \begin{bmatrix}D_1\\ \vdots\\ D_n\\ \vdots\\ D_m\end{bmatrix} + \begin{bmatrix}f_1(\bar{q},\dot{\bar{q}})\\ \vdots\\ f_n(\bar{q},\dot{\bar{q}})\\ \vdots\\ f_m(\bar{q},\dot{\bar{q}})\end{bmatrix}. \tag{8}$$

Lemma 1: Suppose that a positive-definite function $V(t)$ guarantees [40]:

$$\dot{V}(t) \le -\alpha' V(t) - \beta' V^{\rho}(t), \tag{9}$$

where α' and β' are two positive scalars, and ρ is a ratio of two positive numbers with $0 \le \rho \le 1$. Hence, for any initial time t_0, the Lyapunov functional converges to the origin in finite time as

$$t_s = t_0 + \frac{1}{\alpha'(1-\rho)} ln \frac{\alpha' V^{1-\rho}(t_0) + \beta'}{\beta'}. \tag{10}$$

Lemma 2 [41]: If A and B are positive real numbers, then the following inequality is established:

$$(A+B)^{\frac{1}{2}} \le A^{\frac{1}{2}} + B^{\frac{1}{2}}. \tag{11}$$

III. MAIN RESULTS

A. UNDERACTUATED ROBOTIC MANIPULATOR WITH HOLDING

Assumption 1: In this section, it is supposed that the passive joints have holding brakes instead of actuators and therefore they are lockable. Thus,

$$\dot{q}_p = \begin{bmatrix}\dot{q}_{n+1}\\ \vdots\\ \dot{q}_m\end{bmatrix} = \begin{bmatrix}0\\ \vdots\\ 0\end{bmatrix}, \tag{12}$$

$$\ddot{q}_p = \begin{bmatrix}\ddot{q}_{n+1}\\ \vdots\\ \ddot{q}_m\end{bmatrix} = \begin{bmatrix}0\\ \vdots\\ 0\end{bmatrix}, \tag{13}$$

where $q_p \in R^r, \dot{q}_p \in R^r, \ddot{q}_p \in R^r$ signify the positions, velocities and acceleration vectors of passive joints, correspondingly. It is worth noting that since the joint angles are fixed, the velocity and acceleration for the locked joints are equal to zero.

Hence, the active dynamics of underactuated system (8) are presented by:

$$\ddot{q}(t) = M_0 u(t) + D(t) + f(q,\dot{q}), \tag{14}$$

where $u(t) = [u_1 \cdots u_n]^T$, $D(t) = [D_1 \cdots D_n]^T$ and $f(q,\dot{q}) = [f_1(q,\dot{q}) \cdots f_n(q,\dot{q})]^T$; $q \in R^n, \dot{q} \in R^n, \ddot{q} \in R^n$ indicate the position, velocity and acceleration vectors of active joints, respectively.

Assumption 2 [28]: The perturbation vector $D(t)$ is supposed to be norm-bounded as

$$\|D(t)\| \le h, \tag{15}$$

where $h > 0$ is a known constant.

The auxiliary variable is expressed as

$$\delta(t) = z(t) - \dot{q}(t) \tag{16}$$

with $z(t)$ expressed as:

$$\dot{z}(t) = -\varepsilon_0\delta(t) - \varepsilon_1 sign(\delta(t)) + f(q,\dot{q}) + M_0 u(t), \tag{17}$$

where ε_0 and ε_1 are two positive coefficients and $\varepsilon_1 > \|D(t)\|$. The TSM disturbance estimator $\hat{D}(t)$ is proposed by

$$\hat{D}(t) = -\varepsilon_0 \delta(t) - \varepsilon_1 sign(\delta(t)) \tag{18}$$

Theorem 1: Consider the underactuated robotic manipulator (14) and TSM disturbance-observer defined by (16)-(18). Then, the approximation error of the TSMC disturbance observer converges to the equilibrium in the finite time.

Proof: Consider the disturbance approximation error vector defined by:

$$\tilde{D}(t) = \hat{D}(t) - D(t). \tag{19}$$

Taking the time-derivative of (16) and employing (14) and (17) yields:

$$\dot{\delta}(t) = \dot{z}(t) - \ddot{q}(t) = -\varepsilon_0 \delta(t) - \varepsilon_1 sign(\delta(t)) - D(t). \tag{20}$$

Substituting (18) into (20), one obtains

$$\dot{\delta}(t) = \hat{D}(t) - D(t) = \tilde{D}(t). \tag{21}$$

Construct the Lyapunov candidate function as

$$V_1(\delta(t)) = 0.5\delta(t)^T \delta(t) = 0.5\|\delta(t)\|^2. \tag{22}$$

Using (20) and (22), the time-derivative of $V_1(\delta(t))$ is found as

$$\begin{aligned}\dot{V}_1(\delta(t)) &= \delta(t)^T(-\varepsilon_0\delta(t) - \varepsilon_1 sign(\delta(t)) - D(t)) \\ &= -\varepsilon_0\|\delta(t)\|^2 - \varepsilon_1\delta(t)^T sign(\delta(t)) - \delta(t)^T D(t)\end{aligned} \tag{23}$$

Eq. (23) is given by

$$\begin{aligned}\dot{V}_1(\delta(t)) &\le -\varepsilon_0\|\delta(t)\|^2 - \varepsilon_1\|\delta(t)\| - \delta(t)^T D(t) \\ &\le -\varepsilon_0\|\delta(t)\|^2 - \|\delta(t)\|(\varepsilon_1 - \|D\|)\end{aligned} \tag{24}$$

Considering the condition $\varepsilon_1 > \|D(t)\|$, it follows that

$$\dot{V}_1(\delta(t)) \le -\alpha_0 V_1(\delta(t)) - \beta_0 V_1(\delta(t))^{\frac{1}{2}} \tag{25}$$

where $\alpha_0 = 2\varepsilon_0 > 0$ and $\beta_0 = \sqrt{2}(\varepsilon_1 - \|D\|) > 0$.

Based on Lemma 1, Eq. (25) implies that the auxiliary variable $\delta(t)$ converges to the equilibrium in finite time. From (21) and along with the finite-time convergence of the auxiliary variable $\delta(t)$, the error $\tilde{D}(t)$ reaches the origin in finite time. This finalizes the proof. □

The active dynamics of the underactuated system (Eq. (14)) is presumed to track the desired position vector $q_d \in R^n$ and therefore, the tracking errors converge to the origin. The tracking error vector is defined as

$$e(t) = q(t) - q_d(t) \tag{26}$$

where its first and second derivatives are calculated as

$$\dot{e}(t) = \dot{q}(t) - \dot{q}_d(t) \tag{27}$$

$$\begin{aligned}\ddot{e}(t) &= \ddot{q}(t) - \ddot{q}_d(t) \\ \ddot{e}(t) &= \boldsymbol{M_0}u(t) + D(t) + f(q,\dot{q}) - \ddot{q}_d(t).\end{aligned} \tag{28}$$

The GSMC surface $(s(t))$ and non-singular FTSM manifold $(\sigma_1(t))$ are defined as

$$s(t) = e(t) - e(0)\,exp(-\varphi t) \tag{29}$$

$$\sigma_1(t) = s + \mu_1 s^\gamma + \mu_2 \dot{s}^\eta \tag{30}$$

where $\varphi > 0$, $\mu_1 > 0$, $\mu_2 > 0$, $1 < \gamma \le 2$ and $0 < \eta \le 1$.

Theorem 2: Consider the active dynamics of the underactuated system (14) and the designed disturbance observer (16)-(18). If the nonsingular FTSM controller is applied as

$$\begin{aligned}u(t) = \boldsymbol{M_0}^{-1}\Big(&-\frac{1}{\eta\mu_2}\dot{s}^{2-\eta} - \frac{\mu_1\gamma}{\eta\mu_2}s^{\gamma-1}\dot{s}^{2-\eta} - f + \ddot{q}_d - \hat{D} \\ &+ \varphi^2 e(0)\,exp(-\varphi t) + \dot{\delta}(t) \\ &+ \frac{1}{\eta\mu_2}\dot{s}^{1-\eta}(-\varepsilon_0\sigma_1 - \alpha_1 sign(\sigma_1))\Big)\end{aligned} \tag{31}$$

where $\alpha_1 = \varepsilon_1 - h > 0$, then the tracking error (26) and disturbance approximation error (19) converge to the origin.

Proof: From (14), (27) and (29), the first and second derivatives of GSMC surfaces can be obtained as

$$\begin{aligned}\dot{s}(t) &= \dot{e} + \varphi e(0)\exp(-\varphi t) \\ &= \dot{q}(t) - \dot{q}_d(t) + \varphi e(0)\exp(-\varphi t)\end{aligned} \tag{32}$$

$$\begin{aligned}\ddot{s}(t) &= \ddot{q} - \ddot{q}_d - \varphi^2 e(0)\,exp(-\varphi t) \\ &= \boldsymbol{M_0}u + D + f - \ddot{q}_d - \varphi^2 e(0)\,exp(-\varphi t).\end{aligned} \tag{33}$$

Furthermore, in the light of (30)-(33), time-derivative of σ_1 can be obtained as

$$\begin{aligned}\dot{\sigma_1} &= \dot{s} + \mu_1\gamma s^{\gamma-1}\dot{s} + \eta\mu_2\dot{s}^{\eta-1}\ddot{s} \\ &= \dot{s} + \mu_1\gamma s^{\gamma-1}\dot{s} + \eta\mu_2\dot{s}^{\eta-1}(\boldsymbol{M_0}u + D + f - \ddot{q}_d \\ &\quad - \varphi^2 e(0)\,exp(-\varphi t))\end{aligned} \tag{34}$$

Substituting (31) into (34) and using (21) follows that

$$\dot{\sigma_1} = -\varepsilon_0\sigma_1 - \alpha_1 sign(\sigma_1). \tag{35}$$

Construct the Lyapunov candidate functional as

$$V_2(\sigma_1,\delta) = \frac{1}{2}\sigma_1^T\sigma_1 + \frac{1}{2}\delta^T\delta = \frac{1}{2}\|\sigma_1\|^2 + \frac{1}{2}\|\delta\|^2 \tag{36}$$

Differentiating $V_2(\sigma_1,\delta)$ and employing (20) and (35) yields

$$\begin{aligned}\dot{V}_2(\sigma_1,\delta) &= \sigma_1^T\dot{\sigma_1} + \delta^T\dot{\delta} \\ &= \sigma_1^T(-\varepsilon_0\sigma_1 - \alpha_1 sign(\sigma_1)) \\ &\quad + \delta^T(-\varepsilon_0\delta - \varepsilon_1 sign(\delta) - D) \\ &= -\varepsilon_0\|\sigma_1\|^2 - \alpha_1\sigma_1^T sign(\sigma_1) - \varepsilon_0\|\delta\|^2 \\ &\quad - \varepsilon_1\delta^T sign(\delta) - \delta^T D\end{aligned} \tag{37}$$

Considering the fact $\delta^T sign(\delta) \ge \|\delta\|$, Eq. (37) can be written as

$$\begin{aligned}\dot{V}_2(\sigma_1,\delta) &\le -\varepsilon_0\|\sigma_1\|^2 - \alpha_1\|\sigma_1\| - \varepsilon_0\|\delta\|^2 \\ &\quad - \varepsilon_1\|\delta\| - \delta^T D \\ &\le -\varepsilon_0\|\sigma_1\|^2 - \alpha_1\|\sigma_1\| - \varepsilon_0\|\delta\|^2 - (\varepsilon_1 - h)\|\delta\|\end{aligned} \tag{38}$$

where since $\alpha_1 = \varepsilon_1 - h > 0$, one obtains

$$\dot{V}_2(\sigma_1, \delta) \leq -\varepsilon_0 \|\sigma_1\|^2 - \alpha_1 \|\sigma_1\| - \varepsilon_0 \|\delta\|^2 - \varepsilon_1 \|\delta\| - \delta^T D \leq -\varepsilon_0 \left(\|\sigma_1\|^2 + \|\delta\|^2\right) - \alpha_1(\|\sigma_1\| + \|\delta\|) \quad (39)$$

According to Lemma 2, we have

$$-\alpha_1 \|\sigma_1\| - \alpha_1 \|\delta\| \leq -(\alpha_1^2 \|\sigma_1\|^2 + \alpha_1^2 \|\delta\|^2)^{\frac{1}{2}} \quad (40)$$

Substituting (40) into (39) gives

$$\begin{aligned}\dot{V}_2(\sigma_1, \delta) &\leq -\varepsilon_0 \|\sigma_1\|^2 - \alpha_1 \|\sigma_1\| - \varepsilon_0 \|\delta\|^2 - \varepsilon_1 \|\delta\| - \delta^T D \\ &\leq -2\varepsilon_0 \left(\frac{1}{2} \|\sigma_1\|^2 + \frac{1}{2} \|\delta\|^2\right) - \left(\alpha_1^2 \|\sigma_1\|^2 + \alpha_1^2 \|\delta\|^2\right)^{\frac{1}{2}} \\ &= -2\varepsilon_0 \left(\frac{1}{2} \|\sigma_1\|^2 + \frac{1}{2} \|\delta\|^2\right) - \sqrt{2}\alpha_1 \left(\frac{1}{2} \|\sigma_1\|^2 + \frac{1}{2} \|\delta\|^2\right)^{\frac{1}{2}}\end{aligned} \quad (41)$$

where it is clear from (41) that

$$\dot{V}_2(\sigma_1, \delta) \leq -\alpha V_2(\sigma_1, \delta) - \beta V_2(\sigma_1, \delta)^{\frac{1}{2}} \quad (42)$$

This finishes the proof of this theorem. □

Remark 1. In the planned non-singular FTSM manifold (30), it is easy to show that for the case $s < 0$ or $\dot{s} < 0$, the fractional powers $1 < \gamma \leq 2$ and $0 < \eta \leq 1$ lead to the terms $s^\gamma \notin R$ and $\dot{s}^\eta \notin R$.

The modified non-singular FTSM manifold can be proposed to solve the complex-value number problem as

$$\sigma_2 = s + k_1 |s|^{\gamma'} sign(s) + k_2 |\dot{s}|^{\eta'} sign(\dot{s}) \quad (43)$$

where $k_1 > 0$, $k_2 > 0$, $1 < \gamma' \leq 2$ and $0 < \eta' \leq 1$.

Theorem 3: Consider the active dynamics of the underactuated system (14), the non-singular FTSM manifold (43) and the designed disturbance-observer (16)-(18). If the non-singular FTSM control law is applied as

$$\begin{aligned}u_2(t) = \boldsymbol{M}_0^{-1} \Big(&-\frac{1}{\eta' k_2} |\dot{s}|^{1-\eta'} \dot{s} - \frac{k_1 \gamma'}{\eta' k_2} |\dot{s}|^{1-\eta'} |s|^{\gamma'-1} - f + \ddot{q}_d - \hat{D} \\ &+ \varphi^2 e(0) \exp(-\varphi t) + \dot{\delta}(t) \\ &- \frac{1}{\eta' k_2} |\dot{s}|^{1-\eta'} (\varepsilon_0 \sigma_2 + \alpha_1 sign(\sigma_2)) \Big)\end{aligned} \quad (44)$$

where $\alpha_1 = \varepsilon_1 - h > 0$, then the disturbance approximation error (19) and σ_2 converge to zero in the finite time.

Proof: Taking the time-derivative of FTSM manifold (43) yields

$$\dot{\sigma}_2 = \dot{s} + k_1 \gamma' |s|^{\gamma'-1} \dot{s} + k_2 \eta' |\dot{s}|^{\eta'-1} \ddot{s} \quad (45)$$

where substituting (33) into (45) and applying (44) yields

$$\dot{\sigma}_2 = -\varepsilon_0 \sigma_2 - \alpha_1 sign(\sigma_2). \quad (46)$$

Consider the Lyapunov candidate functional as

$$V_3(\sigma_2, \delta) = \frac{1}{2}\sigma_2^T \sigma_2 + \frac{1}{2}\delta^T \delta \quad (47)$$

Calculating the time-derivative of the Lyapunov functional and substituting (20) and (46) gives

$$\dot{V}_3(\sigma_2, \delta) = -\varepsilon_0 \|\sigma_2\|^2 - \alpha_1 \sigma_2^T sign(\sigma_2) - \varepsilon_0 \|\delta\|^2 - \varepsilon_1 \delta^T sign(\delta) - \delta^T D \quad (48)$$

Now, similar to the proof of Theorem 2, we have

$$\begin{aligned}\dot{V}_3(\sigma_2, \delta) &\leq -\varepsilon_0 \|\sigma_2\|^2 - \alpha_1 \|\sigma_2\| - \varepsilon_0 \|\delta\|^2 - \varepsilon_1 \|\delta\| - \delta^T D \\ &\leq -2\varepsilon_0 \left(\frac{1}{2} \|\sigma_2\|^2 + \frac{1}{2} \|\delta\|^2\right) - \left(\alpha_1^2 \|\sigma_2\|^2 + \alpha_1^2 \|\delta\|^2\right)^{\frac{1}{2}} \\ &= -2\varepsilon_0 \left(\frac{1}{2} \|\sigma_2\|^2 + \frac{1}{2} \|\delta\|^2\right) - \sqrt{2}\alpha_1 \left(\frac{1}{2} \|\sigma_2\|^2 + \frac{1}{2} \|\delta\|^2\right)^{\frac{1}{2}}\end{aligned} \quad (49)$$

Finally, the inequality (49) can be written as

$$\dot{V}_3(\sigma_2, \delta) \leq -\alpha" V_3(\sigma_2, \delta) - \beta" V_3(\sigma_2, \delta)^{\frac{1}{2}} \quad (50)$$

where $\alpha" = 2\varepsilon_0$ and $\beta" = \sqrt{2}\alpha_1$. Based on Lemma 1, Eq. (50) shows that the auxiliary variables $\delta(t)$ and σ_2 converge to zero in the finite time. Therefore, the estimation error $\tilde{D}(t)$ reaches the origin in finite time. This finalizes the proof of Theorem 3. □

Remark 2: According to Theorems 1-3, the sliding surface and FTSM manifold converge to zero in finite time. From Eq. (29), it is concluded that if the sliding surface reaches zero, the tracking error $e(t)$ converges to the origin exponentially.

B. UNDERACTUATED ROBOTIC MANIPULATOR WITHOUT HOLDING BRAHES

Assumption 3: In this section, it is supposed that passive joints don't have holding brakes and the joints' velocity and acceleration are not zero. Therefore, considering $\boldsymbol{M'} = \begin{bmatrix} \boldsymbol{M_0} \\ \boldsymbol{M_2} \end{bmatrix} \in R^{m \times n}$, Eq. (8) can be written as

$$\ddot{\bar{q}} = \boldsymbol{M}' u(t) + \bar{D}(t) + \bar{\boldsymbol{f}}\left(\bar{q}, \dot{\bar{q}}\right) \quad (51)$$

The equality (51) is considered as the dynamic equation of the underactuated system.

Assumption 4: The disturbance vector $\bar{D}(t)$ is supposed to be norm-bounded as

$$\left\|\bar{D}(t)\right\| < h_1, \quad (52)$$

where $h_1 > 0$ is an unknown positive constant.

The tracking error vector is defined as

$$e_1(t) = \bar{q}(t) - \bar{q}_d(t) \quad (53)$$

where $\bar{q}_d \in R^m$ is considered as desired position vector.

The GSMC surface ($s_1(t)$) and non-singular FTSM manifold ($\sigma_3(t)$) are defined as

$$s_1(t) = e_1(t) - e_1(0)\,exp(-\varphi t) \tag{54}$$

$$\sigma_3 = s_1 + k_3 |s_1|^{\gamma''} sign(s_1) + k_4 \dot{s}_1 \tag{55}$$

where $\varphi > 0$, $k_4 > 0$, $k_3 > 0$ and $1 < \gamma'' \leq 2$.

The adaptive estimator for h_1 is proposed as

$$\dot{\hat{h}}_1 = k_4 \|\sigma_3\| \tag{56}$$

where the estimation error is defined as

$$\tilde{h}_1 = \hat{h}_1 - h_1. \tag{57}$$

Theorem 4: Consider the dynamic equation of the under-actuated system (51) and the adaptive estimator (56). If the non-singular FTSM controller is applied as

$$\begin{aligned} u_3(t) &= \boldsymbol{M}'^T(\boldsymbol{M}'\boldsymbol{M}'^T)^{-1}(-\bar{f} + \ddot{\bar{q}}_d + \varphi^2 e_1(0)\exp(-\varphi t) \\ &+ \frac{1}{k_4}(-\dot{s}_1 - k_3\gamma'' |s_1|^{\gamma''-1}\dot{s}_1 \\ &- k_4 sign(\sigma_3)\hat{h}_1 - k_5 sign(\sigma_3))), \end{aligned} \tag{58}$$

with

$$k_5 = k_4\left(\sigma_3^T sign(\sigma_3) - \|\sigma_3\|\right) \tag{59}$$

then, the variables $\tilde{h}_1$ and σ_3 converge to zero and it can be concluded that the tracking error $e_1(t)$ is converged to zero.

Proof: The first and second derivatives of $s_1(t)$ are obtained as follows

$$\begin{aligned} \dot{s}_1(t) &= \dot{e}_1 + \varphi e_1(0)\,exp(-\varphi t) \\ &= \dot{\bar{q}}(t) - \dot{\bar{q}}_d(t) + \varphi e_1(0)\,exp(-\varphi t) \end{aligned} \tag{60}$$

$$\begin{aligned} \ddot{s}_1(t) &= \ddot{\bar{q}} - \ddot{\bar{q}}_d - \varphi^2 e_1(0)\,exp(-\varphi t) \\ &= \boldsymbol{M}'u + \bar{D} + \bar{f} - \ddot{\bar{q}}_d - \varphi^2 e_1(0)\,exp(-\varphi t) \end{aligned} \tag{61}$$

Then, taking the time-derivative of FTSM manifold (55) and substituting $\ddot{s}_1$ and u_3 into it, yields

$$\dot{\sigma}_3 = -k_4 sign(\sigma_3)\hat{h}_1 + k_4\bar{D} - k_5 sign(\sigma_3) \tag{62}$$

Consider the Lyapunov candidate functional as

$$V_4(\sigma_3, \tilde{h}_1) = \frac{1}{2}\sigma_3^T\sigma_3 + \frac{1}{2}\tilde{h}_1^2 \tag{63}$$

Taking the time-derivative of the Lyapunov functional and using $\dot{\sigma}_3$ and $\dot{\tilde{h}}_1 = \dot{\hat{h}}_1$ gives

$$\begin{aligned} \dot{V}_4\left(\sigma_3, \tilde{h}_1\right) &= \sigma_3^T\left(-k_4 sign(\sigma_3)\hat{h}_1 + k_4\bar{D} - k_5 sign(3)\right) \\ &\quad + \tilde{h}_1(k_4\|\sigma_3\|), \end{aligned} \tag{64}$$

The above equation can be written as

$$\begin{aligned} \dot{V}_4\left(\sigma_3, \tilde{h}_1\right) \leq &-k_4\sigma_3^T sign(\sigma_3)\hat{h}_1 + k_4\|\sigma_3\|\left\|\bar{D}\right\| \\ &- k_4\|\sigma_3\| h_1 \\ &- k_5\|\sigma_3\| + \tilde{h}_1(k_4\|\sigma_3\|) + k_4\|\sigma_3\| h_1 \end{aligned} \tag{65}$$

where since $\hat{h}_1 = h_1 + \tilde{h}_1$, then we have

$$\begin{aligned} \dot{V}_4\left(\sigma_3, \tilde{h}_1\right) \leq &-k_4 h_1\left(\sigma_3^T sign(\sigma_3) - \|\sigma_3\|\right) \\ &- k_4\|\sigma_3\|\left(h_1 - \left\|\bar{D}\right\|\right) \\ &- k_5\|\sigma_3\| - k_4\left(\sigma_3^T sign(\sigma_3) - \|\sigma_3\|\right)\tilde{h}_1 \end{aligned} \tag{66}$$

From (59) and (66), one obtains

$$\dot{V}_4\left(\sigma_3, \tilde{h}_1\right) \leq -k_5\|\sigma_3\| - k_5\tilde{h}_1 \tag{67}$$

The above inequality can be written as

$$\begin{aligned} \dot{V}_4\left(\sigma_3, \tilde{h}_1\right) &\leq -\sqrt{2}k_5\left(\frac{1}{2}\|\sigma_3\|^2 + \frac{1}{2}\tilde{h}_1^2\right)^{\frac{1}{2}} \\ &= -\beta_{01}V_4\left(\sigma_3, \tilde{h}_1\right)^{\frac{1}{2}} \end{aligned} \tag{68}$$

where $\beta_{01} = \sqrt{2}k_5$; $\tilde{h}_1$ and σ_3 converge to zero, and therefore the tracking error $e_1(t)$ is convergent to zero. The proof of Theorem 4 is finished. □

IV. SIMULATION RESULTS

A. IMPLEMENTATION TO AN UNDERACTUATED MANIPULATOR WITH HOLDING BRAKES

In this section, the proposed non-singular FTSM control law (44) is implemented to a 3-link robotic manipulator which third joint is passive, and hence has a holding brake and is locked as illustrated in Fig. 1.

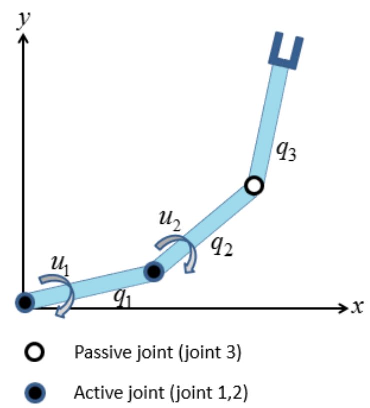

FIGURE 1. Configuration of underactuated 3-link robot manipulator.

Consider the dynamics of a 3-link robotic manipulator as follows:

$$\boldsymbol{B}\begin{bmatrix}\ddot{q}_1\\ \ddot{q}_2\\ \ddot{q}_3\end{bmatrix} + \boldsymbol{C}\begin{bmatrix}\dot{q}_1\\ \dot{q}_2\\ \dot{q}_3\end{bmatrix} + f_d\begin{bmatrix}\dot{q}_1\\ \dot{q}_2\\ \dot{q}_3\end{bmatrix} + f_s\begin{bmatrix}sgn(\dot{q}_1)\\ sgn(\dot{q}_2)\\ sgn(\dot{q}_3)\end{bmatrix} + \tau_1\begin{bmatrix}1\\ 1\\ 1\end{bmatrix} + \begin{bmatrix}g_1(q)\\ g_2(q)\\ g_3(q)\end{bmatrix} = \begin{bmatrix}u_1(t)\\ u_2(t)\\ u_3(t)\end{bmatrix}, \tag{69}$$

with $B = \begin{bmatrix} b_{11} & b_{12} & b_{13}\\ b_{21} & b_{22} & b_{23}\\ b_{31} & b_{32} & b_{33}\end{bmatrix}$, $C = \begin{bmatrix} h_{11} & h_{12} & h_{13}\\ h_{21} & h_{22} & h_{23}\\ h_{31} & h_{32} & h_{33}\end{bmatrix}$.

where:

$$b_{11} = I_{l_1} + m_{l_1}l_1^2 + k_{r_1}^2 I_{m_1} + I_{l_2} + m_{m_2}a_1^2 + I_{m_2} + I_{l_3} + I_{m_3}$$

$$+m_{l_2}\left(a_1^2+l_2^2+2a_1l_2c_2\right)$$
$$+m_{m_3}\left(a_1^2+a_2^2+2a_1a_2c_1\right)$$
$$+m_{l_3}\left(a_1^2+a_2^2+l_3^2+2a_1a_2c_2+2a_1l_3c_{23}+2a_2l_3c_3\right) \quad (70)$$

$$b_{22}=I_{l_2}+I_{l_3}+k_{r_2}^2I_{m_2}+I_{m_3}+m_{m_3}a_2^2+m_{l_2}I_2^2+m_{l_3}\left(a_2^2+l_3^2+2a_2l_3c_3\right), \quad (71)$$

$$b_{33}=I_{l_3}+k_{r_3}^2I_{m_3}+m_{l_3}l_3^2, \quad (72)$$

$$b_{12}=b_{21}=I_{l_2}+I_{l_3}+k_{r_2}I_{m_2}+I_{m_3}+m_{m_3}\left(a_2^2+a_1a_2c_2\right)+m_{l_2}\left(l_2^2+a_1l_2c_2\right)+m_{l_3}\left(a_2^2+l_3^2+a_1a_2c_2+a_1l_3c_{23}+2a_2l_3c_3\right) \quad (73)$$

$$b_{13}=b_{31}=I_{l_3}+k_{r_3}I_{m_3}+m_{l_3}\left(l_3^2+a_1l_3c_{23}+a_2l_3c_3\right) \quad (74)$$

$$b_{23}=b_{32}=I_{l_3}+k_{r_3}I_{m_3}+m_{l_3}\left(l_3^2+a_2l_3c_3\right) \quad (75)$$

$$h_{11}=-m_{m_3}a_1a_2s_1\dot{q}_1-\left(m_{l_3}a_1l_3s_{23}+m_{l_3}a_2l_3s_3\right)\dot{q}_3-\left(m_{l_2}+m_{l_3}a_1a_2s_2+a_1l_2s_2+m_{l_3}a_1l_3s_{23}\right)\dot{q}_2 \quad (76)$$

$$h_{22}=-\left(m_{l_3}a_2l_3s_3\right)\dot{q}_3 \quad (77)$$

$$h_{33}=-\left(m_{l_3}a_1a_2s_2\right)\dot{q}_2-\left(m_{l_3}a_2l_3s_3\right)\dot{q}_3 \quad (78)$$

$$h_{12}=-\left(m_{l_2}a_1l_2s_2+m_{l_3}a_1l_3s_{23}+m_{l_3}a_1a_2s_2\right)\dot{q}_1-\left(m_{l_3}a_1a_2s_2+m_{l_3}a_1l_3s_{23}+m_{m_3}a_1a_2s_2+m_{l_2}a_1l_2s_2\right)\dot{q}_2-\left(m_{l_3}a_2l_3s_3+m_{l_3}a_1l_3s_{23}\right)\dot{q}_3 \quad (79)$$

$$h_{13}=-\left(m_{l_3}a_1l_3s_{23}+m_{l_3}a_2l_3s_3\right)\dot{q}_1-\left(m_{l_3}a_1l_3s_{23}+m_{l_3}a_2l_3s_3\right)\dot{q}_2-\left(m_{l_3}a_2l_3s_2+m_{l_3}a_1l_3s_{23}\right)\dot{q}_3 \quad (80)$$

$$h_{21}=\left(m_{l_2}a_1l_2s_2+m_{l_3}a_1a_2s_2+m_{l_3}a_1l_3s_{23}\right)\dot{q}_1-\left(m_{l_3}a_2l_3s_3\right)\dot{q}_3 \quad (81)$$

$$h_{23}=-\left(m_{l_3}a_2l_3s_3\right)\dot{q}_1-\left(m_{l_3}a_2l_3s_3\right)\dot{q}_2-\left(m_{l_3}a_2l_3s_3\right)\dot{q}_3 \quad (82)$$

$$h_{31}=\left(m_{l_3}a_1l_3s_{23}+m_{l_3}a_2l_3s_3\right)\dot{q}_1+\left(m_{l_3}a_2l_3s_3\right)\dot{q}_2 \quad (83)$$

$$h_{32}=\left(m_{l_3}a_2l_3s_3\right)\dot{q}_1+\left(m_{l_3}a_2l_3s_3\right)\dot{q}_2-\left(m_{l_3}a_2l_3s_3\right)\dot{q}_3 \quad (84)$$

$$g_1(q)=\left(m_{l_2}l_2+m_{m_3}a_2+m_{l_3}a_2\right)gc_{12}+m_{l_3}l_3gc_{123}+\left(m_{l_1}I_1+m_{l_3}a_1+m_{l_2}a_1+m_{m_2}a_1+m_{m_3}a_1\right)gc_1 \quad (85)$$

$$g_2(q)=\left(m_{l_2}l_2+m_{l_3}a_2+m_{m_3}a_2\right)gc_{12}+m_{l_3}l_3gc_{123} \quad (86)$$

$$g_3(q)=m_{l_3}l_3gc_{123} \quad (87)$$

with: $c_1=cos(q_1)$, $s_1=\sin(q_1)$, $c_2=\cos(q_2)$, $s_2=\sin(q_2)$, $c_{12}=cos(q_1+q_2)$, $c_3=\cos(q_3)$, $c_{123}=cos(q_1+q_2+q_3)$, $s_{123}=sin(q_1+q_2+q_3)$, $s_{12}=sin(q_1+q_2)$.

Let l_1, l_2 and l_3 be the distances of the mass centers of three links from their joint axis, m_{l_1}, m_{l_2} and m_{l_3} be the links' masses, m_{m_1}, m_{m_2} and m_{m_3} be the rotors' masses, I_{l_1}, I_{l_2} and I_{l_3} be the moments of inertia of the links, and I_{m_1}, I_{m_2} and I_{m_3} be the rotors' moments of inertia. The constant parameters are taken as $m_{m_2}=m_{m_3}=m_{m_1}=1kg$, $a_1=a_2=1$, $l_1=l_2=l_3=0.5m$, $m_{l_1}=m_{l_2}=m_{l_3}=10kg$, $I_{l_1}=I_{l_2}=I_{l_3}=1kg.m^2$, $I_{m_1}=I_{m_2}=I_{m_3}=1kg.m^2$, $k_{r_1}=k_{r_2}=k_{r_3}=1$, $f_s=f_d=0.001$, $\tau_1=1$.

From(69), the dynamics of underactuated 3-link robotic manipulator is considered as

$$\ddot{q}=\begin{bmatrix}\ddot{q}_1\\ \ddot{q}_2\\ \ddot{q}_3\end{bmatrix}=\boldsymbol{B}^{-1}\begin{bmatrix}u_1\\ u_2\\ 0\end{bmatrix}+\begin{bmatrix}D_1\\ D_2\\ D_3\end{bmatrix}+\begin{bmatrix}f_1(\overline{q},\dot{\overline{q}})\\ f_2(\overline{q},\dot{\overline{q}})\\ f_3(\overline{q},\dot{\overline{q}})\end{bmatrix}, \quad (88)$$

where it is assumed that $\dot{q}_3=0$ and $\ddot{q}_3=0$, and

$$\begin{bmatrix}f_1(\overline{q},\dot{\overline{q}})\\ f_2(\overline{q},\dot{\overline{q}})\\ f_3(\overline{q},\dot{\overline{q}})\end{bmatrix}=-\boldsymbol{B}^{-1}\left(\boldsymbol{C}\begin{bmatrix}\dot{q}_1\\ \dot{q}_2\\ 0\end{bmatrix}+\begin{bmatrix}g_1\\ g_2\\ g_3\end{bmatrix}\right), \quad (89)$$

$$\begin{bmatrix}D_1\\ D_2\\ D_3\end{bmatrix}=-\boldsymbol{B}^{-1}\left(\begin{bmatrix}f_s\, sign(q_1)\\ f_s\, sign(q_2)\\ f_s\, sign(q_3)\end{bmatrix}+f_d\begin{bmatrix}\dot{q}_1\\ \dot{q}_2\\ 0\end{bmatrix}+\begin{bmatrix}\tau_1\\ \tau_1\\ \tau_1\end{bmatrix}\right). \quad (90)$$

The active dynamic model of the underactuated system is stated from (88) by

$$\ddot{q}=\begin{bmatrix}\ddot{q}_1\\ \ddot{q}_2\end{bmatrix}=\boldsymbol{M_0}\begin{bmatrix}u_1\\ u_2\end{bmatrix}+\begin{bmatrix}D_1\\ D_2\end{bmatrix}+\begin{bmatrix}f_1(q,\dot{q})\\ f_2(q,\dot{q})\end{bmatrix}. \quad (91)$$

where $\boldsymbol{M_0}\in R^{2\times 2}$ is a sub-matrix of $\boldsymbol{B}^{-1}=\begin{bmatrix}\boldsymbol{M_0} & \boldsymbol{M_1}\\ \boldsymbol{M_2} & \boldsymbol{M_3}\end{bmatrix}$. The proposed non-singular FTSM control law(44) is applied to (91) and the parameters of the proposed control approach are selected as $\eta'=1$, $\gamma'=\frac{5}{3}$, $k_1=1$, $k_2=0.4$, $\varphi=2$, $\varepsilon_0=2$, $\varepsilon_1=5.2$, $\alpha_1=2.9$ and $h=2.3$. The initial conditions are set as $q_1(0)=0.5$, $q_2(0)=0$, $q_3(0)=0$, $\dot{q}_1(0)=0$, $\dot{q}_2(0)=0$ and the desired position vector is chosen as $q_d=\begin{bmatrix}sin(2\pi t)\\ sin(2\pi t)\end{bmatrix}$. The convergenc time of the sliding surfaces can be obtained by the following procedure:

Using the initial conditions, one obtains $e(0)=\begin{bmatrix}0.5\\ 0\end{bmatrix}$. By substituting $e(0), \dot{q}_d(0)=\begin{bmatrix}2\pi\\ 2\pi\end{bmatrix}, \dot{q}(0)=\begin{bmatrix}0\\ 0\end{bmatrix}$ and $\varphi=2$ into Eq.(32), we have $\dot{s}(0)=\dot{q}(0)-\dot{q}_d(0)+\varphi e(0)=\begin{bmatrix}-2\pi\\ -2\pi\end{bmatrix}+2\begin{bmatrix}0.5\\ 0\end{bmatrix}=\begin{bmatrix}-5.28\\ -6.28\end{bmatrix}$. Then, by substituting $s(0)=0$, $\dot{s}(0)=\begin{bmatrix}-5.28\\ -6.28\end{bmatrix}$, $k_1=1$, $k_2=0.4$, $\eta'=1$, $\gamma'=\frac{5}{3}$ into (43), we attain $\sigma_2(0)$ as $\sigma_2(0)=s(0)+k_1|s(0)|^{\gamma'}sign(s(0))+k_2|\dot{s}(0)|^{\eta'}sign(\dot{s}(0))=0.4\left|\begin{bmatrix}-5.28\\ -6.28\end{bmatrix}\right|sign\left(\begin{bmatrix}-5.28\\ -6.28\end{bmatrix}\right)=\begin{bmatrix}-2.11\\ -2.51\end{bmatrix}$. Using (16), one has $\delta(0)=z(0)-\dot{q}(0)=\begin{bmatrix}1\\ 1\end{bmatrix}$. As a result, based on Eq. (47), $V_3(0)$ is calculated as $V_3(0)=\frac{1}{2}\sigma_2^T(0)\sigma_2(0)+\frac{1}{2}\delta^T(0)\delta(0)=6.38$. According to Lemma 1 and considering

$t_0 = 0, \beta" = \sqrt{2}\alpha_1 = 4.10$ and $\alpha" = 2\varepsilon_0 = 4$, the convergence time is obtained as $t_{1s} = \frac{1}{\alpha"(0.5)} ln \frac{\alpha" V_3^{0.5}(0)+\beta"}{\beta"} = \frac{1}{4(0.5)} ln \frac{4\times 6.38^{0.5}+4.1}{4.1} = 0.62$.

Fig. 2 highlights the tracking performance of the joint positions, which shows that the joint positions track the reference trajectories appropriately. The corresponding tracking errors are depicted in Fig. 3. Note the convergence of the errors to the equilibrium in finite-time. The time histories of the auxiliary variables, GSMC surfaces and non-singular FTSM manifolds are illustrated in Fig. 4. It is obvious from Fig. 4 that the sliding manifolds converge to the equilibrium in finite time as well.

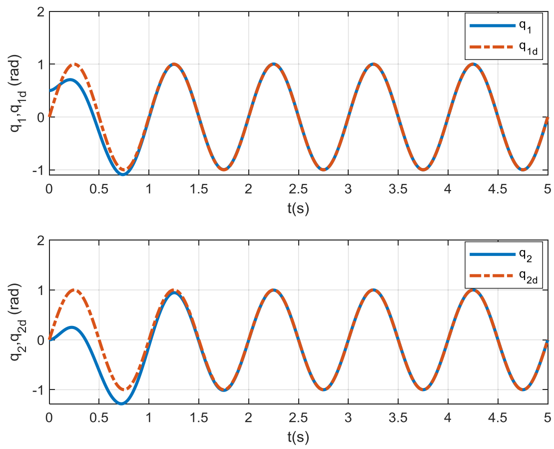

FIGURE 2. Time responses of joint positions.

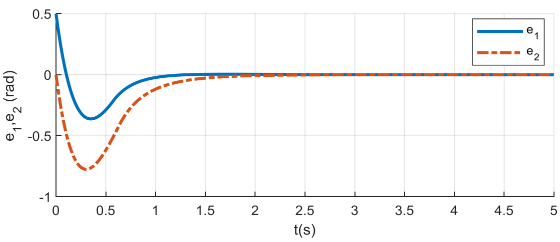

FIGURE 3. Time histories of the tracking errors.

According to the above simulation results, one can confirm that the proposed control methodology was able to achieve acceptable dynamic response of the underactuated robotic manipulator in the presence of external disturbances.

To further assess the robustness of the proposed approach, we modify the external disturbance, desired position vector and initial conditions as follows: $\tau_1 = cos(0.2\pi t)$, $q_d = \begin{bmatrix} sin(2\pi t) \\ cos(2\pi t) \end{bmatrix}$, $q_1(0) = 0.5, q_2(0) = 0.5, q_3(0) = 1, \dot{q}_1(0) = 0, and \dot{q}_2(0) = 0$.

The convergence time of the sliding surfaces with the above considered conditions can be computed by the following procedure: by substituting $e(0) = \begin{bmatrix} 0.5 \\ -0.5 \end{bmatrix}$, $\dot{q}_d(0) = \begin{bmatrix} 2\pi \\ 0 \end{bmatrix}$, $\dot{q}(0) = \begin{bmatrix} 0 \\ 0 \end{bmatrix}$ and $\varphi = 2$ into Eq. (32), we have $\dot{s}(0) = \dot{q}(0) - \dot{q}_d(0) + \varphi e(0) = \begin{bmatrix} -2\pi \\ 0 \end{bmatrix} + 2\begin{bmatrix} 0.5 \\ -0.5 \end{bmatrix} = \begin{bmatrix} -5.28 \\ -1 \end{bmatrix}$. Then, by substituting $s(0) = 0, \dot{s}(0) = \begin{bmatrix} -5.28 \\ -1 \end{bmatrix}, k_1 = 1, k_2 = 0.4, \eta' = 1, \gamma' = \frac{5}{3}$ into (43), we can obtain $\sigma_2(0)$ as $\sigma_2(0) = s(0) + k_1 |s(0)|^{\gamma'} sign(s(0)) + k_2 |\dot{s}(0)|^{\eta'} sign(\dot{s}(0)) = 0.4\left|\begin{bmatrix} -5.28 \\ -1 \end{bmatrix}\right| sign\left(\begin{bmatrix} -5.28 \\ -1 \end{bmatrix}\right) = \begin{bmatrix} -2.11 \\ -0.4 \end{bmatrix}$. From (16), one obtains $\delta(0) = z(0) - \dot{q}(0) = \begin{bmatrix} 1 \\ 1 \end{bmatrix}$. As a result, based on Eq. (47), $V_3(0)$ is found as $V_3(0) = \frac{1}{2}\sigma_2^T(0)\sigma_2(0) + \frac{1}{2}\delta^T(0)\delta(0) = 3.3$. Now, considering $t_0 = 0, \beta" = \sqrt{2}\alpha_1 = 4.10, \alpha" = 2\varepsilon_0 = 4$, the convergence time is calculated as

$$t_{2s} = \frac{1}{\alpha"(0.5)} ln \frac{\alpha" V_3^{0.5}(0) + \beta"}{\beta"} = \frac{1}{4(0.5)} ln \frac{4 \times 3.3^{0.5} + 4.1}{4.1} = 0.51.$$

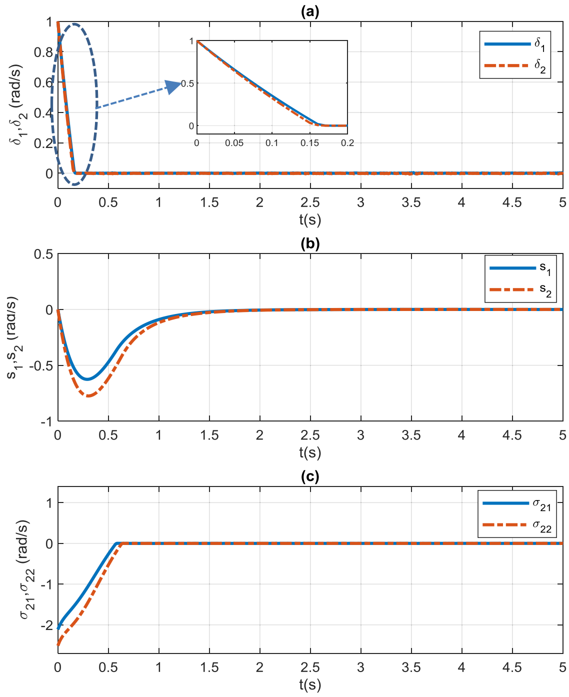

FIGURE 4. (a)Auxiliary variables, (b) GSMC surfaces, (c) non-singular FTSM.

Fig. 5 depicts the time responses of the joint positions, which confirms the system's good tracking performance. Fig. 6 shows the dynamics of the tracking errors and confirm their finite-time convergence to the origin. Fig. 7 highlights the time trajectories of the auxiliary variables, GSMC surfaces and non-singular FTSM manifolds. It is obvious from these plots that the GSMC surfaces and non-singular FTSM manifolds approach the equilibrium in finite time. Fig. 8 shows the control inputs of the robotic manipulator. Note that fast and excellent tracking performance is achieved without the use of large feedback gains.

One can conclude from the above results that the proposed controller yields acceptable tracking performance in

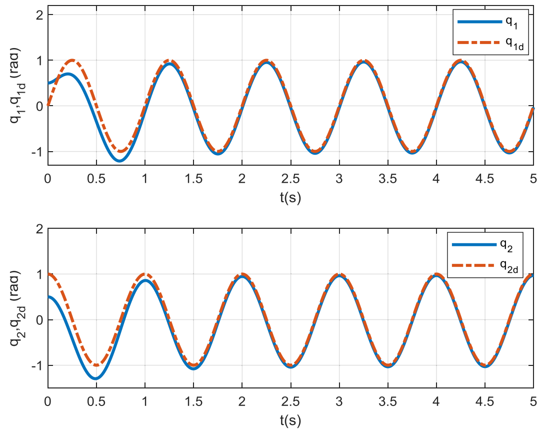

FIGURE 5. Time histories of the joint positions.

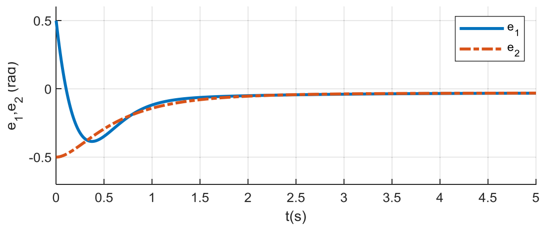

FIGURE 6. Time histories of the tracking errors.

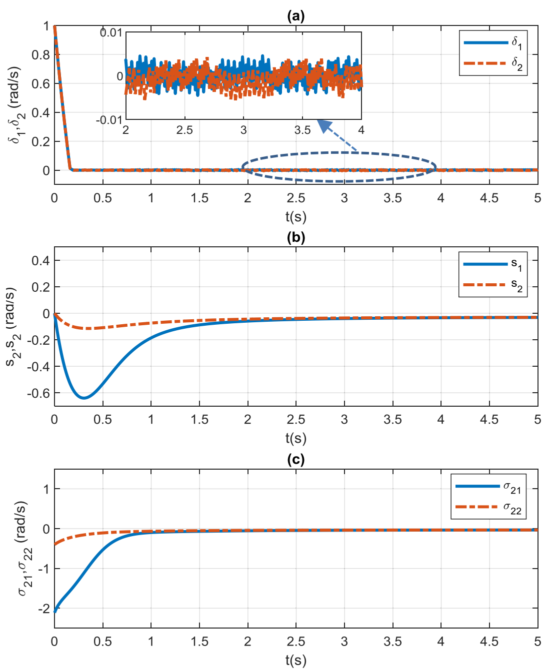

FIGURE 7. (a) Auxiliary variables, (b) GSMC surfaces, (c) non-singular FTSM.

the presence of several external disturbances and under various initial conditions and desired position vectors.

B. IMPLEMENTATION TO AN UNDERACTUATED MANIPULATOR WITHOUT HOLDING BRAKES

In this section, the robotic manipulator without holding brakes is considered. Using Eq. (88) and substituting the terms $\bar{f}\left(\bar{q},\dot{\bar{q}}\right) = \left[f_1(\bar{q},\dot{\bar{q}})f_2(\bar{q},\dot{\bar{q}})f_3(\bar{q},\dot{\bar{q}})\right]^T, u\left(t\right) =$

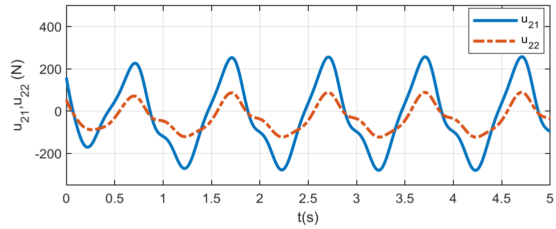

FIGURE 8. Control inputs.

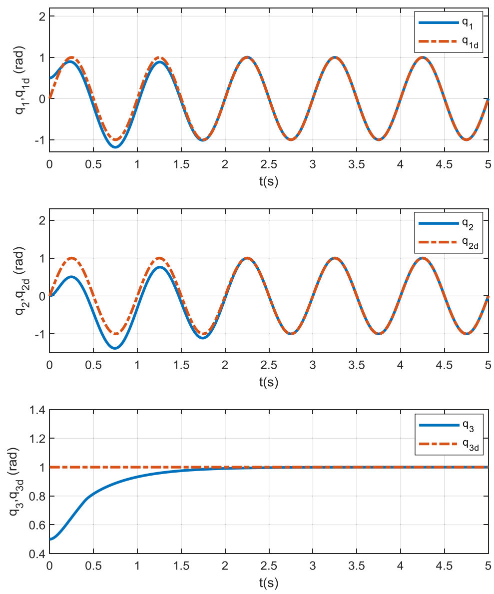

FIGURE 9. Time responses of the joint positions.

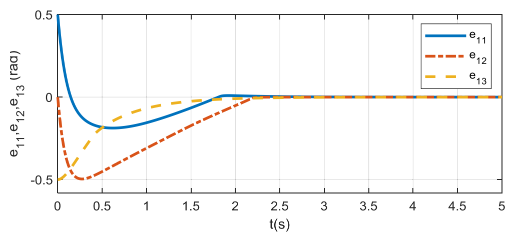

FIGURE 10. Time histories of the tracking errors.

$[u_1 u_2]^T, \bar{D}\left(t\right) = [D_1 D_2 D_3]^T, \boldsymbol{B}^{-1} = \begin{bmatrix} \boldsymbol{M_0} & \boldsymbol{M_1} \\ \boldsymbol{M_2} & \boldsymbol{M_3} \end{bmatrix} \in R^{3\times 3}$ and $\boldsymbol{M}' = \begin{bmatrix} \boldsymbol{M_0} \\ \boldsymbol{M_2} \end{bmatrix}$, one can have:

$$\ddot{\bar{q}} = \begin{bmatrix} \ddot{q}_1 \\ \ddot{q}_2 \\ \ddot{q}_3 \end{bmatrix} = \boldsymbol{M}'u + \bar{D}\left(t\right) + \bar{f}\left(\bar{q},\dot{\bar{q}}\right) \tag{92}$$

The proposed non-singular FTSM control law (58) is applied to Eq. (92) and the parameters of the suggested control input are selected as $\gamma'' = 9/7, k_3 = 5, k_4 = 0.1, \varphi = 2$. The initial conditions are also chosen as $q_1\left(0\right) = 0.5, q_2\left(0\right) = 0, q_3\left(0\right) = 0.5, \dot{q}_1\left(0\right) = 0, \dot{q}_2\left(0\right) = 0, \dot{q}_3\left(0\right) = 0$ and the desired position vector and disturbance term are specified as

$$\bar{q}_d = \begin{bmatrix} sin\left(2\pi t\right) \\ sin(2\pi t) \\ 1 \end{bmatrix} \quad \text{and } \tau_1 = 0.5.$$

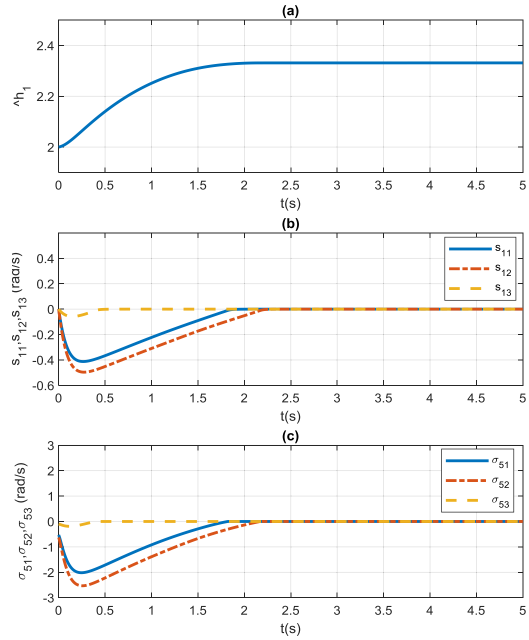

FIGURE 11. **(a) Estimation of h_1, (b) GSMC surfaces, (c) non-singular FTSM manifolds.**

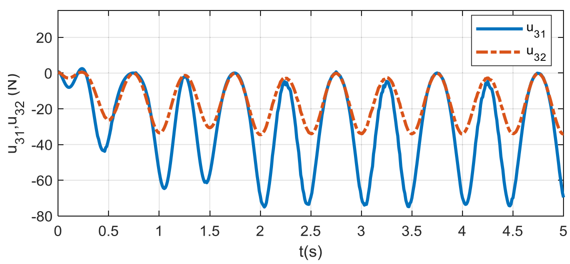

FIGURE 12. **Control inputs.**

Fig. 9 shows the time responses of the joint positions, which demonstrates the appropriate tracking performance of the joint positions. Fig. 10 depicts the time histories of the tracking errors, which shows the convergence of these signals to the origin. Fig. 11 exhibits the time trajectories of the estimation of h_1, GSMC surfaces and non-singular FTSM manifolds. It is obvious from these plots that the GSMC surfaces and non-singular FTSM manifolds quickly converge to the origin. Fig. 12 displays the control inputs of the underactuated robotic manipulator.

One can conclude from the above results that the proposed controller exhibits good tracking performance for the underactuated robot manipulator without holding brakes, in the presence of external disturbance with unknown bound.

V. CONCLUSION

This paper proposed a fast non-singular terminal sliding controller based on disturbance observer and adaptive estimator for the tracking control of underactuated robotic manipulators with unknown bounded external disturbances. The proposed control scheme is derived based on a novel non-singular FTSM manifold that solves the singularity and complex-value number problems typically associated with standard SMC. The performance of the proposed control approach was assessed using an underactuated robotic manipulators with and without holding brakes. The obtained results showed that the proposed NSFTSM guaranteed zero-tracking errors for the position joints, whereas the disturbance observer ensured the finite-time convergence of the approximation error to the origin for various disturbance levels, initial conditions and desired position levels. In our future work, we will focus on practically implementing the design to a robot manipulator and assessing its performance.

APPENDIX

Proof of Lemma 1: If two sides of inequality (9) are divided to $V^{\rho}(t)$, we obtain

$$V^{-\rho}(t)\dot{V}(t) \leq -\alpha' V^{1-\rho}(t) - \beta' \tag{93}$$

and thus,

$$dt \leq -\frac{V^{-\rho}(t)}{\alpha' V^{1-\rho}(t) + \beta'} dV(t) \tag{94}$$

Integrating two sides of (94) from t_0 to t_s yields

$$\begin{aligned} t_s - t_0 &\leq -\int_{V(t_0)}^{0} \frac{V^{-\rho}(t)}{\alpha' V^{1-\rho}(t) + \beta'} dV(t) \\ &= -\frac{1}{\alpha'(1-\rho)} \{\ln \beta' - \ln\left(\alpha' V^{1-\rho}(t_0) + \beta'\right)\} \\ &= \frac{1}{\alpha'(1-\rho)} ln \frac{\alpha' V^{1-\rho}(t_0) + \beta'}{\beta'} \end{aligned} \tag{95}$$

REFERENCES

[1] S. Mobayen, "Design of LMI-based sliding mode controller with an exponential policy for a class of underactuated systems," *Complexity*, vol. 21, no. 5, pp. 117–124, May 2016.
[2] N. Sun and Y. Fang, "New energy analytical results for the regulation of underactuated overhead cranes: An end-effector motion-based approach," *IEEE Trans. Ind. Electron.*, vol. 59, no. 12, pp. 4723–4734, Dec. 2012.
[3] K. Shojaei and M. Dolatshahi, "Line-of-sight target tracking control of underactuated autonomous underwater vehicles," *Ocean Eng.*, vol. 133, pp. 244–252, Mar. 2017.
[4] I. Tortopidis and E. Papadopoulos, "Point-to-point planning: Methodologies for underactuated space robots," in *Proc. IEEE Int. Conf. Robot. Autom.*, May 2006, pp. 3861–3866.
[5] M.-D. Hua, T. Hamel, P. Morin, and C. Samson, "A control approach for thrust-propelled underactuated vehicles and its application to VTOL drones," *IEEE Trans. Autom. Control*, vol. 54, no. 8, pp. 1837–1853, Aug. 2009.
[6] S. Riachy, Y. Orlov, T. Floquet, R. Santiesteban, and J.-P. Richard, "Second-order sliding mode control of underactuated mechanical systems I: Local stabilization with application to an inverted pendulum," *Int. J. Robust Nonlinear Control*, vol. 18, nos. 4–5, pp. 529–543, 2008.
[7] B. Roy and H. H. Asada, "Nonlinear feedback control of a gravity-assisted underactuated manipulator with application to aircraft assembly," *IEEE Trans. Robot.*, vol. 25, no. 5, pp. 1125–1133, Oct. 2009.
[8] K. A. Hamed, B. G. Buss, and J. W. Grizzle, "Continuous-time controllers for stabilizing periodic orbits of hybrid systems: Application to an underactuated 3D bipedal robot," in *Proc. IEEE Conf. Decis. Control*, Dec. 2014, pp. 1507–1513.
[9] B. Belzile and L. Birglen, "Stiffness analysis of underactuated fingers and its application to proprioceptive tactile sensing," *IEEE/ASME Trans. Mechatronics*, vol. 21, no. 6, pp. 2672–2681, Dec. 2016.
[10] R. Muñoz-Mansilla, D. Chaos, J. M. Díaz, and J. Aranda, "Application of quantitative feedback theory techniques for the control of a non-holonomic underactuated hovercraft," *IET Control Theory Appl.*, vol. 6, no. 14, pp. 2188–2197, Sep. 2012.

[11] G. Rigatos and K. Busawon, "Underactuated robotic manipulators," in *Robotic Manipulators Vehicles*. Cham, Switzerland: Springer, 2018, pp. 65–159.
[12] M. Chignoli and P. M. Wensing, "Variational-based optimal control of underactuated balancing for dynamic quadrupeds," *IEEE Access*, vol. 8, pp. 49785–49797, 2020.
[13] M. W. Spong, "Energy based control of a class of underactuated mechanical systems," *IFAC Proc. Volumes*, vol. 29, no. 1, pp. 2828–2832, Jun. 1996.
[14] R. Olfati-Saber, "Normal forms for underactuated mechanical systems with symmetry," *IEEE Trans. Autom. Control*, vol. 47, no. 2, pp. 305–308, 2002.
[15] J. Huang, S. Ri, T. Fukuda, and Y. Wang, "A disturbance observer based sliding mode control for a class of underactuated robotic system with mismatched uncertainties," *IEEE Trans. Autom. Control*, vol. 64, no. 6, pp. 2480–2487, Jun. 2019.
[16] M. Steinberger, M. Horn, and L. Fridman, *Variable-Structure Systems and Sliding-Mode Control*. New York, NY, USA: Springer, 2020.
[17] S. Mobayen and F. Tchier, "A novel robust adaptive second-order sliding mode tracking control technique for uncertain dynamical systems with matched and unmatched disturbances," *Int. J. Control, Autom. Syst.*, vol. 15, no. 3, pp. 1097–1106, Jun. 2017.
[18] X. Xi, S. Mobayen, H. Ren, and S. Jafari, "Robust finite-time synchronization of a class of chaotic systems via adaptive global sliding mode control," *J. Vib. Control*, vol. 24, no. 17, pp. 3842–3854, 2017.
[19] J.-J. Xiong and G.-B. Zhang, "Global fast dynamic terminal sliding mode control for a quadrotor UAV," *ISA Trans.*, vol. 66, pp. 233–240, Jan. 2017.
[20] J. J. Rath, M. Defoort, H. R. Karimi, and K. C. Veluvolu, "Output feedback active suspension control with higher order terminal sliding mode," *IEEE Trans. Ind. Electron.*, vol. 64, no. 2, pp. 1392–1403, Feb. 2017.
[21] C. U. Solis, J. B. Clempner, and A. S. Poznyak, "Fast terminal sliding-mode control with an integral filter applied to a van der pol oscillator," *IEEE Trans. Ind. Electron.*, vol. 64, no. 7, pp. 5622–5628, Jul. 2017.
[22] J. Ni, L. Liu, C. Liu, X. Hu, and S. Li, "Fast fixed-time nonsingular terminal sliding mode control and its application to chaos suppression in power system," *IEEE Trans. Circuits Syst. II, Exp. Briefs*, vol. 64, no. 2, pp. 151–155, Feb. 2017.
[23] L. Yang and J. Yang, "Nonsingular fast terminal sliding-mode control for nonlinear dynamical systems," *Int. J. Robust Nonlinear Control*, vol. 21, no. 16, pp. 1865–1879, Nov. 2011.
[24] Y. Feng, X. Yu, and Z. Man, "Non-singular terminal sliding mode control of rigid manipulators," *Automatica*, vol. 38, no. 12, pp. 2159–2167, Dec. 2002.
[25] S. H. Lee, J. B. Park, and Y. H. Choi, "Finite time control of nonlinear underactuated systems using terminal sliding surface," in *Proc. IEEE Int. Symp. Ind. Electron. (ISIE)*, Jul. 2009, pp. 626–631.
[26] X. Wang and S. Li, "Finite-time trajectory tracking control of underactuated autonomous surface vessels based on non-singular terminal sliding mode," *Austral. J. Electr. Electron. Eng.*, vol. 9, no. 3, pp. 235–246, Jan. 2012.
[27] X. Huang, Y. Yan, Y. Zhou, and D. Hao, "Fast terminal sliding mode control of underactuated spacecraft formation reconfiguration," *J. Aerosp. Eng.*, vol. 29, no. 5, Sep. 2016, Art. no. 04016020.
[28] Q. Khan, R. Akmeliawati, A. I. Bhatti, and M. A. Khan, "Robust stabilization of underactuated nonlinear systems: A fast terminal sliding mode approach," *ISA Trans.*, vol. 66, pp. 241–248, Jan. 2017.
[29] G. Zhang, C. Zhang, T. Yang, and W. Zhang, "Disturbance observer-based composite neural learning path following control of underactuated ships subject to input saturation," *Ocean Eng.*, vol. 216, Nov. 2020, Art. no. 108033.
[30] X. Wu, K. Xu, and X. He, "Disturbance-observer-based nonlinear control for overhead cranes subject to uncertain disturbances," *Mech. Syst. Signal Process.*, vol. 139, May 2020, Art. no. 106631.
[31] D. Belleter, M. A. Maghenem, C. Paliotta, and K. Y. Pettersen, "Observer based path following for underactuated marine vessels in the presence of ocean currents: A global approach," *Automatica*, vol. 100, pp. 123–134, Feb. 2019.
[32] B. Lu, Y. Fang, and N. Sun, "Sliding mode control for underactuated overhead cranes suffering from both matched and unmatched disturbances," *Mechatronics*, vol. 47, pp. 116–125, Nov. 2017.
[33] W. Chen, Y. Wei, J. Zeng, H. Han, and X. Jia, "Adaptive terminal sliding mode NDO-based control of underactuated AUV in vertical plane," *Discrete Dyn. Nature Soc.*, vol. 2016, Jan. 2016, Art. no. 6590517.
[34] Q. Hou, S. Ding, and X. Yu, "Composite super-twisting sliding mode control design for PMSM speed regulation problem based on a novel disturbance observer," *IEEE Trans. Energy Convers.*, early access, Apr. 6, 2020, doi: 10.1109/TEC.2020.2985054.
[35] Y. Wu, B. Jiang, and N. Lu, "A descriptor system approach for estimation of incipient faults with application to high-speed railway traction devices," *IEEE Trans. Syst., Man, Cybern., Syst.*, vol. 49, no. 10, pp. 2108–2118, Oct. 2019.
[36] Y. Wu, B. Jiang, and Y. Wang, "Incipient winding fault detection and diagnosis for squirrel-cage induction motors equipped on CRH trains," *ISA Trans.*, vol. 99, pp. 488–495, Apr. 2020.
[37] P. Sánchez-Sánchez and M. A. Arteaga-Pérez, "Simplied methodology for obtaining the dynamic model of robot manipulators," *Int. J. Adv. Robot. Syst.*, vol. 9, no. 5, p. 170, 2012.
[38] M. W. Spong and M. Vidyasagar, *Robot Dynamics and Control*. Hoboken, NJ, USA: Wiley, 2008.
[39] S. Mobayen, F. Tchier, and L. Ragoub, "Design of an adaptive tracker for n-link rigid robotic manipulators based on super-twisting global nonlinear sliding mode control," *Int. J. Syst. Sci.*, vol. 48, no. 9, pp. 1990–2002, Mar. 2017.
[40] E. Moulay and W. Perruquetti, "Finite time stability and stabilization of a class of continuous systems," *J. Math. Anal. Appl.*, vol. 323, no. 2, pp. 1430–1443, Nov. 2006.
[41] S. Yu, X. Yu, B. Shirinzadeh, and Z. Man, "Continuous finite-time control for robotic manipulators with terminal sliding mode," *Automatica*, vol. 41, no. 11, pp. 1957–1964, Nov. 2005.

SALEH MOBAYEN (Member, IEEE) received the B.Sc. and M.Sc. degrees in control engineering from the University of Tabriz, Tabriz, Iran, in 2007 and 2009, respectively, and the Ph.D. degree in control engineering from Tarbiat Modares University, Tehran, Iran, in January 2013. From February 2013 to December 2018, he was an Assistant Professor and a Faculty Member with the Department of Electrical Engineering, University of Zanjan, Zanjan, Iran, where he has also been an Associate Professor of control engineering with the Department of Electrical Engineering, since December 2018. He is currently with the Future Technology Research Center, National Yunlin University of Science and Technology, as an Associate Professor. His research interests include control theory, sliding mode control, robust tracking, non-holonomic robots, and chaotic systems.

SOHEILA MOSTAFAVI was born in Hamedan, Iran, in September 1994. She received the B.S. degree in electrical engineering from the University of Kurdistan, Kurdistan, Iran, in 2016, and the M.Sc. degree in control engineering from the University of Zanjan, Zanjan, Iran, in 2018. Her research interests include robust control, nonlinear systems, linear matrix inequality, and sliding mode control.

AFEF FEKIH (Senior Member, IEEE) received the B.S., M.S., and Ph.D. degrees in electrical engineering from the National Engineering School of Tunis, Tunisia, in 1995, 1998, and 2002, respectively. She is currently a Full Professor with the Department of Electrical and Computer Engineering and a Chevron/BORSF Professor in engineering with the University of Louisiana at Lafayette. Her research interests include control theory and applications, including nonlinear and robust control, optimal control, fault tolerant control with applications to power systems, wind turbines, unmanned vehicles, and automotive engines.